Mine Water Environ
DOI 10.1007/s10230-016-0384-6

TECHNICAL ARTICLE

Sorption Testing and Generalized Composite Surface Complexation Models for Determining Uranium Sorption Parameters at a Proposed In-situ Recovery Site

Raymond H. Johnson[1] · Ryan A. Truax[2] · David A. Lankford[3] · James J. Stone[2]

Received: 25 February 2015 / Accepted: 20 January 2016

Abstract Solid-phase iron concentrations and generalized composite surface complexation models were used to evaluate procedures in determining uranium sorption on oxidized aquifer material at a proposed U in situ recovery (ISR) site. At the proposed Dewey Burdock ISR site in South Dakota, USA, oxidized aquifer material occurs downgradient of the U ore zones. Solid-phase Fe concentrations did not explain our batch sorption test results, though total extracted Fe appeared to be positively correlated with overall measured U sorption. Batch sorption test results were used to develop generalized composite surface complexation models that incorporated the full generic sorption potential of each sample, without detailed mineralogic characterization. The resultant models provide U sorption parameters (site densities and equilibrium constants) for reactive transport modeling. The generalized composite surface complexation sorption models were calibrated to batch sorption data from three oxidized core samples using inverse modeling, and gave larger sorption parameters than just U sorption on the measured solid-phase Fe. These larger sorption parameters can significantly influence reactive transport modeling, potentially increasing U attenuation. Because of the limited number of calibration points, inverse modeling required the reduction of estimated parameters by fixing two parameters. The best-fit models used fixed values for equilibrium constants, with the sorption site densities being estimated by the inversion process. While these inverse routines did provide best-fit sorption parameters, local minima and correlated parameters might require further evaluation. Despite our limited number of proxy samples, the procedures presented provide a valuable methodology to consider for sites where metal sorption parameters are required. These sorption parameters can be used in reactive transport modeling to assess downgradient metal attenuation, especially when no other calibration data are available, such as at proposed U ISR sites.

Keywords Geochemical modeling · Batch sorption · PHREEQC · PEST

Introduction

Alkaline solutions are injected into the subsurface to leach U from ore in sandstones as part of the in situ recovery (ISR) process. Reactive aqueous solutions are prepared by addition of oxidants, such as oxygen, and anionic carbonate species, such as carbon dioxide or sodium bicarbonate, which enhance the solubility of the oxidized U. Uranium generally occurs as U(IV) within the chemically reducing ore zones, but the U(IV) is converted to the more soluble U(VI) by the oxidizing conditions of the ISR process. Uranium mobility can be attenuated by sorption, which is kept low by the use of the carbonate complexing agents. Injection and pumping wells are used to circulate the

Electronic supplementary material The online version of this article (doi:10.1007/s10230-016-0384-6) contains supplementary material, which is available to authorized users.

✉ Raymond H. Johnson
ray.johnson@lm.doe.gov

[1] Navarro Research and Engineering, Contractor to the U.S. Department of Energy Office of Legacy Management, 2597 Legacy Way, Grand Junction, CO 81503, USA

[2] Department of Civil and Environmental Engineering, South Dakota School of Mines and Technology, 501 East Saint Joseph Str, Rapid City, SD 57701, USA

[3] Naval Nuclear Power Pipeline, U.S. Navy, Washington, DC, USA

Published online: 03 February 2016

oxygen and complexing agents and bring the soluble U in the "pregnant lixiviant" to the surface for removal from solution. After U removal, the "barren lixiviant" is reused. Once the U is largely recovered from the ore zone, the same injection and pumping wells are used to recirculate clean water in an attempt to remove excess dissolved constituents, residual oxidants, and soluble U. Depending on site conditions, other restoration methods, such as groundwater sweeping and using restoration fluids other than clean water, might be used to reestablish reducing conditions and remove U from the groundwater. Several sources (e.g. Commonwealth of Australia 2010; IAEA 2005; NRC 2009) provide general information on U ISR methods and restoration practices. ISR methods avoid the environmental issues associated with traditional open-pit or underground mining. However, U ISR operations are generally conducted in productive groundwater aquifers, some of which may be shared aquifers used for a potable water source laterally away from the ISR operations. Because of implications to water quality, post-ISR aquifer restoration is an important issue.

In general, initial licenses/permits for companies in the USA proposing U ISR require aquifer restoration to pre-ISR conditions or better. However, groundwater restoration to pre-ISR chemistry for all constituents is difficult (Hall 2009; Davis and Curtis 2007), which has led to the use of alternate concentration limits (ACLs) for various constituents, including U (EPA 2011 provides some examples). The justification for these ACLs has generally been based on groundwater classification standards (e.g. industrial water supply, animal stock water). However, any groundwater constituent that remains above pre-ISR concentrations may be considered a contaminant if it migrates past the site boundaries. Thus, protection of aquifers downgradient of ISR zones is a long-term concern once natural groundwater flow conditions are reestablished.

The U.S. Environmental Protection Agency (EPA) regulations specifically state that U ISR facilities must have an approved aquifer exemption permit, which specifies that no change in groundwater geochemistry should occur outside of the aquifer exemption boundary. While this applies to all groundwater constituents, U is generally considered the main contaminant of concern. Sorption of U (which can be reversible) on downgradient solid-phase aquifer materials is a possible natural attenuation mechanism, but due to limited monitoring data at U ISR sites after restoration, this process has not been well documented (Borch et al. 2012).

Generally, U ISR focuses on roll-front deposits that form in permeable sandstones. Through geologic time, as U is solubilized with oxygenated groundwater, it is precipitated at a redox front. The downgradient solid phase generally contains organic carbon or pyrite, or both, which can act as reductants for dissolved U and create conditions in which the U is less mobile. Over time, this U roll-front moves downward along the hydraulic gradient; depending on the balance of oxygen to the available reductants, the concentration of solid-phase U sometimes increases to economically recoverable amounts (Adler 1974; Boberg 2010; Harshman 1974; Hobday and Galloway 1999). After U ISR is complete, any U transported into the downgradient reducing zone is likely sorbed or precipitated, forming a "new" U roll-front deposit. In some cases, changes in the groundwater flow direction through geologic time can create conditions in which the downgradient solid phase is the oxidized portion of the original roll-front deposit. Under these conditions, any soluble U remaining in an ISR zone may be attenuated by the remaining iron oxyhydroxides and any other U-sorbing materials, since reducing agents are not present. In this setting, natural attenuation of U by sorption on iron oxyhydroxides is likely to be less effective as potential attenuation processes within the reduced zone, creating concerns for downgradient U transport within the oxidized zone. This unique scenario occurs in parts of the proposed U ISR zones at the Dewey Burdock site, near Edgemont South Dakota, USA, which is the subject of this study. More details on this scenario are provided in a companion paper by Johnson and Tutu (2016).

For proposed U ISR sites, no downgradient U plume exists and, due to this lack of plume calibration data, predictive reactive transport models must rely on laboratory U sorption capacity determinations. Several studies have described U sorption on a variety of mineral surfaces (Bachmaf and Merkel 2011; Nair et al. 2014; Pabalan et al. 1998; Villalobos et al. 2001; Waite et al. 1994). Much of the previous literature focused specifically on U sorption to iron oxyhydroxides (Dzombak and Morel 1990; Hsi and Langmuir 1985; Mahoney et al. 2009; Waite et al. 1994), as iron oxyhydroxides effectively sorb many different metals. However, more recent research (e.g. Davis et al. 2004) has led to the development of generalized composite surface complexation models that present a more generic approach that is independent of the actual sorbent. This approach is especially useful when detailed mineralogy is not available.

The goal of this work was to evaluate appropriate procedures for determining U sorption parameters for use in simulating natural attenuation of U downgradient of a proposed U ISR site. We present a method for evaluating solid-phase iron concentrations, batch sorption tests, and construction of generalized composite surface complexation models for an improved determination of sorption capacities for use in reactive transport modeling. Reactive transport modeling for U specific to the Dewey Burdock site is provided elsewhere in this issue (Johnson and Tutu 2016), using the sorption parameters from this paper. The

limited number of samples used here does not provide definitive data for use in final quantitative site sorption capacities and reactive transport modeling, but do provide data to inform methodologies for use in future studies. While the data in this paper are specific to the proposed Dewey Burdock U ISR site, the methods and procedures can potentially be applied to other sites where U and other metal sorption on downgradient solid-phase materials is a consideration.

Dewey Burdock Site

The proposed Dewey Burdock ISR site is located near Edgemont, South Dakota, USA, in a historical U-mining district. Surface mining has depleted the most easily accessible, shallow U deposits; however, a series of deeper U roll-front deposits have been identified as ISR-amenable future resources (NRC 2014; Powertech 2008, 2009).

Ideally, core material from directly downgradient of proposed U ISR zones would be available for analysis, characterization, and sorption testing. Representative downgradient core samples from the Dewey Burdock site were not available, so oxidized core material with a low U content from previously drilled ore zone cores were used as proxy materials. These cores likely have similar mineralogy to what would be expected in areas downgradient of the proposed ISR. The oxidized core material was from either above or below the U ore zones, within a core drilled to identify ore; details on the core locations are provided in Johnson et al. (2013).

For this study, we evaluated four oxidized zone core samples for U sorption capacity using new data on extractable Fe content and batch sorption tests with laboratory-created aqueous solutions (Supplemental Table A-1) that were similar to the native groundwater, to test the hypothesis that U sorption occurs mainly on iron oxyhydroxides. Johnson (2012) and Johnson et al. (2013) provide previous groundwater and solid-phase data, respectively, for the Dewey Burdock site. All of the samples were from the lower Chilson Member of the Lakota Formation, which is part of the Inyan Kara Group. The lower Chilson is composed of siliceous, fine- to medium-grained fluvial sandstones that are somewhat consolidated. The U deposits occur at the contact of oxidized zones with reduced carbonaceous sandstones. Dahlkamp (2010) presents a thorough summary of U deposits in the area. X-ray diffraction (XRD) data on the oxidized sandstone samples indicate 96–97 % quartz, a trace to 2 % kaolinite, 2–4 % potassium feldspar, and up to 1 % hematite (Johnson et al. 2013). Independent of site mineralogy and site specifics, the focus of this study was to evaluate potential U sorption in downgradient oxidized zones, as an industry-relevant approach with broad application. A companion paper (Johnson and Tutu 2016) provides more details on the Dewey Burdock site hydrogeology and rock/water interactions downgradient of the ore zones, coupled with reactive transport modeling.

Methods

Iron Extractions

Sequential iron extractions with progressively stronger extraction fluids were used to qualitatively determine the amount of amorphous Fe (dissolved with weaker extraction fluids) compared to more crystalline Fe (dissolved with stronger extraction fluids). The extraction steps discussed below are presented in order of weaker to stronger extraction fluids. First, we lightly disaggregated rock samples with a mortar and pestle; no sieving or further processing was required due to minor cementation. Chemical extractions for iron were modified slightly from those of Heron et al. (1994). Approximately 5 g of sediment was combined with 40 mL of 0.5 N HCl in an amber glass serum vial that was purged with nitrogen gas. The sediment was reacted for 24 h with intermittent agitation by hand to suspend the sediment; then, an aliquot of the resulting solution was removed using a needle and syringe. The withdrawn solution was immediately filtered through a 0.2 μm syringe filter and reacted with orthophenanthroline, according to the procedure of Clesceri et al. (1998), to determine ferrous and total dissolved Fe concentrations. This extraction is referred to as the HCl extraction step. The remaining sediment in the amber glass serum vial was subsequently recovered by filtration (0.45 μm), rinsed thoroughly with distilled water, and air dried overnight.

The residual sediment was then combined with a 40 mL solution of 1.4 M NH_2OH in 1 M HCl in a polyethylene tube and reacted for 24 h with periodic hand shaking, after which the same procedures described above were used to determine the total content of dissolved Fe (Clesceri et al. 1998). This extraction is referred to as the NH_2OH–HCl extraction step. The remaining sediment was subsequently recovered by filtration (0.45 μm), rinsed thoroughly with distilled water, and air-dried overnight.

A 1.5 g aliquot of the air-dried residue from the NH_2-OH–HCl extraction was weighed, placed in an amber glass serum vial, and combined with 40 mL of 0.008 M titanous chloride ($Ti^{3+}Cl^{3-}$) in 0.05 M disodium ethylenediaminetetraacetic acid (EDTA). The pH of the combined solution was adjusted to between 6 and 6.5 using sodium hydroxide. The Ti^{3+}–EDTA solution was prepared and introduced into an amber glass serum vial under nitrogen

gas. The serum vial was sealed, purged with nitrogen for 3 min, wrapped with foil, and shaken intermittently by hand over the 24 h reaction period. Then, 30 mL of the solution was removed through the septum using a needle and syringe and filtered with a 0.2 μm syringe filter. The Ti^{3+}–EDTA solution has a medium-intensity magenta color prior to reaction with ferric iron. This color was apparent, although less intense, at the completion of the reaction, indicating that the Ti^{3+} was not completely consumed during reaction with the sediment. The filtered solution was then analyzed for total Fe using the Ferrozine reagent of Hach Chemical Company. This extraction is referred to as the Ti^{3+}–EDTA extraction step. Although the sediment was dried in air prior to evaluation of reducible Fe, the readily reactive Fe phases were removed by the 0.5 N HCl prior to air exposure, and any remaining reduced Fe phases, such as pyrite, react slowly and contribute little to the Ti^{3+}–EDTA extraction (Heron et al. 1994).

Additional Fe data included a total sample digestion to provide a total Fe value for each sample and information on hematite content using XRD. Johnson et al. (2013) describes the methods and provides the reported data.

Simulated Groundwater Preparation

For the batch sorption tests, actual site groundwater was not available, so a groundwater analysis from a well completed at core location 11-14C within the ore zone of the lower Chilson member of the Lakota Formation (well 684, Johnson 2012) was used. This sample is representative of the groundwater in the local area where the cores were collected (Johnson 2012; Johnson et al. 2013) and had a similar geochemistry to four other sampling events (Powertech 2009). The geochemical modeling program PHREEQC (Parkhurst and Appelo 2013) was used to calculate how a laboratory-prepared water could be created to match the geochemistry of the original groundwater. The resulting calculation provided a reasonable substitute for the major cations and anions in the groundwater solution by dissolving laboratory-grade $MgSO_4$, (0.5774 g), Na_2SO_4 (1.57 g), and $NaHCO_3$ (0.022 g) in 1 L of deionized water. The groundwater at the Dewey Burdock site is generally anoxic. However, due to the use of oxidized core material and the possibility that post-restoration groundwater in the ore zone may contain some residual oxygen, the laboratory–prepared water was created using laboratory deionized water without any oxygen control. For the batch sorption testing, the laboratory-prepared water was spiked with three different amounts of uranyl nitrate to produce U concentrations of 0.607, 1.22, and 2.32 mg/L. Supplemental Table A-1 provides the complete solution chemistry of the laboratory-prepared water samples (B series).

Batch Sorption Tests

Batch sorption tests used splits of the samples from the iron extractions after light disaggregation with a mortar and pestle. For each batch test, 20 g of sample was added to a 60 mL, acid-washed, amber glass serum vial. Each solid-phase sample was analyzed with four separate batch tests using the laboratory-prepared water (see previous section), a zero-U-concentration solution, and the three U-spiked solutions. For each test, between 50 and 53 mL of laboratory-prepared water was added along with 0.5 mL of 0.16 N H_2SO_4, which was used to adjust the pH between 6 and 7. The capped serum vials trapped CO_2, which maintained pCO_2 at values similar to those in the aquifer (approximately-1.5 log pCO_2, in atmospheres).

The vials were sealed with butyl rubber septa and crimp rings and agitated periodically by hand for 48 h, at ambient laboratory temperature. Chemical equilibrium was assumed to occur by 48 h based on relatively fast U sorption on iron oxyhydroxides (Fox et al. 2006; Waite et al. 1994). After 48 h, the vials were opened and the pH was measured by inserting a pH probe into the vial (which may have increased K and Ag concentrations from the electrode). The solution was then drawn from the vial and filtered through a 0.2 μm filter. A 25 mL aliquot of the filtrate was placed in an acid-washed HDPE bottle and acidified with high-purity HNO_3 for ICP-MS analysis. A second aliquot was used for alkalinity determination.

For each spiked U concentration, the difference in concentration between the spiked amount and the final concentration after 48 h was used to calculate the amount of U sorbed to the solid phase. These results assumed that the oxidizing conditions of the batch tests had inhibited precipitation, an assumption that was confirmed with geochemical modeling, except for sample 11-14C-3 (discussed later). However, the initial batch test with no U in solution often desorbed some existing U from the solid-phase sample, as the laboratory-prepared solutions equilibrated with the solid samples. The amount of U desorbed with the zero-U-spiked solution provided a minimum pre-existing base sorption, where base sorption refers to the amount of U sorbed to the solid phase before the addition of any laboratory-prepared solutions. The base sorption calculated from the zero-U-solution batch test was added to the sorption calculated from the three additional U-spiked batch tests.

Modeling of U Sorption on Iron Oxyhydroxides

Sorption of U onto iron oxyhydroxide was simulated using PHREEQC, which along with other geochemical modeling programs, use the Dzombak and Morel (1990) database for metal sorption on iron oxyhydroxides. This database was

created using extensive laboratory testing of sorption of a variety of metals onto a generic hydrous ferric oxide (HFO as FeOOH). Dzombak and Morel (1990) did not test U specifically in the laboratory, but instead modeled sorption parameters for U after the results from other metals.

In PHREEQC, parameters for Fe in the solid phase were entered directly, along with an assumed surface area of 600 m^2, which is the default value in PHREEQC (Parkhurst and Appelo 2013) based on previous iron oxyhydroxide sorption studies. We entered data for the total extracted and total Fe concentrations into PHREEQC along with the matching water geochemistry for each batch sorption test to calculate a simulated amount of sorbed U. Each simulation assumed equilibrium with the water phase; PHREEQC calculates all of the associated U complexes that would keep U in solution and thereby inhibit sorption. The PHREEQC database used in this study included recently updated U thermodynamics, U complexation, and HFO sorption parameters provided by Guillaumont et al. (2003), Dong and Brooks (2006), and Mahoney et al. (2009), respectively. The updated database is included in Supplemental Exhibit A-2.

Inverse Modeling Procedures for Batch Sorption Test Calibration

The geochemical model PHREEQC was used to model the geochemical conditions of each batch sorption test with the presumption that all of the sorption surfaces can be represented using a composite property (see Supplemental Exhibit A-3). The following equations for a generalized composite surface complexation model (Davis et al. 2004) were added to PHREEQC.

$$SSOH + UO_2^{2+} = SSOUO_2^{+} + H^{+} \quad (1)$$

$$SOH + UO_2^{2+} = SOUO_2^{+} + H^{+} \quad (2)$$

These equations include strong (S) and super-strong (SS) sorption sites for U. Weak sites were not included to reduce the number of parameters to be estimated, as preliminary tests indicated very low sensitivities to the weak site parameters. The sorption parameters for estimation were the log k (equilibrium constant) and sorption site density for each equation, for a total of four parameters.

The four parameters, S log k, SS log k, S site density, and SS site density, can be estimated manually using simple trial and error to match the measured sorption curves. However, the use of an automated calibration routine like PEST (Parameter ESTimation, Doherty 2005) provides additional information on goodness of fit for the calibration, parameter and calibration data sensitivities, and provides information on parameter correlations. Routines like PEST continually adjust each parameter slightly, rerun the simulation program, and provide a final best-fit calibration based on achieving the smallest sum-of-squares weighted residual (SOSWR) value. The SOSWR values are calculated by taking the difference between all of the observed and simulated values, squaring those values, and then adding them together (Doherty 2005). The residuals are also weighted as necessary based on the magnitude of the different parameters to allow for cross-parameter comparisons.

As a general rule in inverse modeling, the number of parameters being estimated should be less than the number of observations (Poeter and Hill 1997). Initial testing with PEST indicated that using three parameters or more created convergence problems. For each sample, the three different U concentrations are the only three observation points. Since four parameters had to be estimated, two parameters had to be fixed to constant values. Three simulations were performed: (1) fix the log k values and estimate the site densities, (2) fix the site densities and estimate the log k values, and (3) fix the ratio of the two log k values and fix the ratio of the two site densities. In (3), the ratio values were determined based on the final estimated values in (1) and (2). The SOSWR values from these three approaches were then compared to assess the best goodness of fit. The starting values for the fixed parameters of log k in (1) and site densities in (2) used values from Davis et al. (2004). Although Davis et al. (2004) evaluated a different site, the oxidized river material they used was similar in grain size and mineralogy to the material at the Dewey Burdock site and provided reasonable starting parameters.

Results and Discussion

Solid-Phase Iron Concentrations

Table 1 provides data on the sequential Fe extractions, total extracted Fe, and the total Fe in each sample. Additional data on these samples include a complete whole rock acid digestion analyzed with ICP-MS for 55 elements, XRD analyses, and petrographic analyses of thin sections (Johnson et al. 2013). Overall variations in the whole rock and XRD data showed only minor differences among the four samples (Johnson et al. 2013). All of the oxidized samples were red and contained no pyrite or organic carbon. Sample 11-14C-5 had the highest total Fe content but the lowest percent of extractable Fe. Sample 11-16C-2 had the highest amount of extractable Fe. From the XRD data, sample 11-14C-5 had 1 % hematite, and sample 11-16C-2 may have contained some hematite (below the 1 % detection limit). The hematite detected in sample 11-14C-5 is consistent with the higher total Fe content (Table 1), and the slightly lower hematite content in sample 11-16C-2

Table 1 Solid-phase extracted and total iron concentrations

Sample	HCl ferrous mg/kg	HCl ferric mg/kg	NH_2OH–HCl Fe mg/kg	Ti^{3+}-EDTA Fe mg/kg	Total extracted Fe mg/kg	Total Fe mg/kg	Fe, as extracted %
11-14C-3	44.0	80.0	120	360	604	999	60.5
11-14C-4	17.0	123	150	609	899	2350	38.3
11-14C-5	34.0	180	78.0	800	1092	4270	25.6
11-16C-2	41.0	259	300	1130	1730	3940	43.9

may be due to a larger amount of amorphous Fe that was also more extractable (Table 1). The presence of hematite is a possibility for all of these oxidized samples, but the quantities were too low for good quantitative XRD detection. Visible Fe staining and some Fe-oxide cement in thin sections (Fig. 1) were present in all of the samples. Thus, Table 1 shows the best quantitative measure of Fe content, and these values were used to model U sorption with the total extracted and total Fe contents (discussed below).

Batch Sorption Tests and Modeled U Sorption on Iron Oxyhydroxides

Table 2 provides batch sorption test results, and Figs. 2, 3 and 4 are graphs of measured and modeled sorption for samples 11-14C-4, 11-14C-5, and 11-16C-2, respectively, using the same scale for U sorption. The differences in U concentration in solution relative to the starting concentration indicates the amount sorbed to the solid phase and is

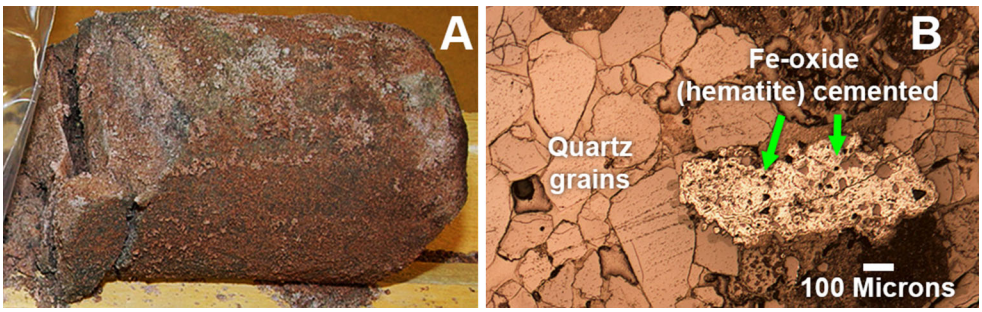

Fig. 1 **a** Photograph of oxidized core, approximately 15 cm long. **b** Thin section of sample 11–14C–5 showing iron oxides

Table 2 Data from uranium sorption batch tests

Sample	Initial dissolved U mg/L	Final dissolved U mg/L	Dissolved U gain (+)/loss (−) mg/L	U sorbed on solid phase[b] mg/kg	Total U sorbed mg/kg	K_d^b L/kg
11-14C-4-1	0.00	0.0938	0.0938	−0.235	0.235	
11-14C-4-2	0.607	0.406	−0.201	0.503	0.737	1.21
11-14C-4-3	1.22	0.841	−0.379	0.948	1.18	0.97
11-14C-4-4	2.32	1.85	−0.470	1.18	1.41	0.61
11-14C-5-1	0.00	0.447	0.447	−1.12	1.12	
11-14C-5-2	0.607	0.607	0.00	0.00	1.12	1.84
11-14C-5-3	1.22	0.944	−0.276	0.690	1.81	1.48
11-14C-5-4	2.32	1.60	−0.720	1.80	2.92	1.26
11-16C-2-1	0.00	0.0552	0.0552	−0.138	0.138	
11-16C-2-2	0.607	0.214	−0.393	0.983	1.12	1.85
11-16C-2-3	1.22	0.250	−0.970	2.43	2.56	2.10
11-16C-2-4	2.32	0.902	−1.42	3.55	3.68	1.59

Sample 11-14C-3 sorption data are not presented due to likely mineral precipitation (see text)

[a] Negative value for uranium sorbed on solid phase indicates desorption, which is used as a base sorption amount (see text)

[b] K_d = sorption coefficient = total uranium sorbed divided by final uranium in solution

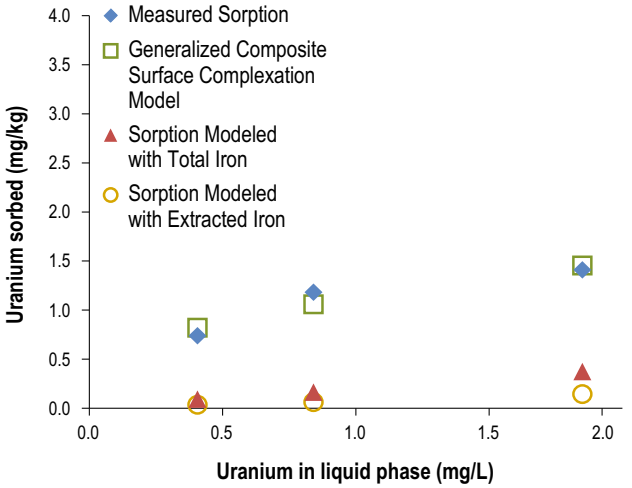

Fig. 2 Measured and modeled sorption for 11–14C–4. A *blue diamond symbol* represents the measured sorption data where the uranium in the liquid phase is plotted as the final uranium in solution from Table 2. A *red triangle* represents the modeled uranium sorption based on the total iron content, and a *yellow circle* represents the modeled uranium sorption based on the total extracted iron content. The *green square* represents results from the generalized composite surface complexation models

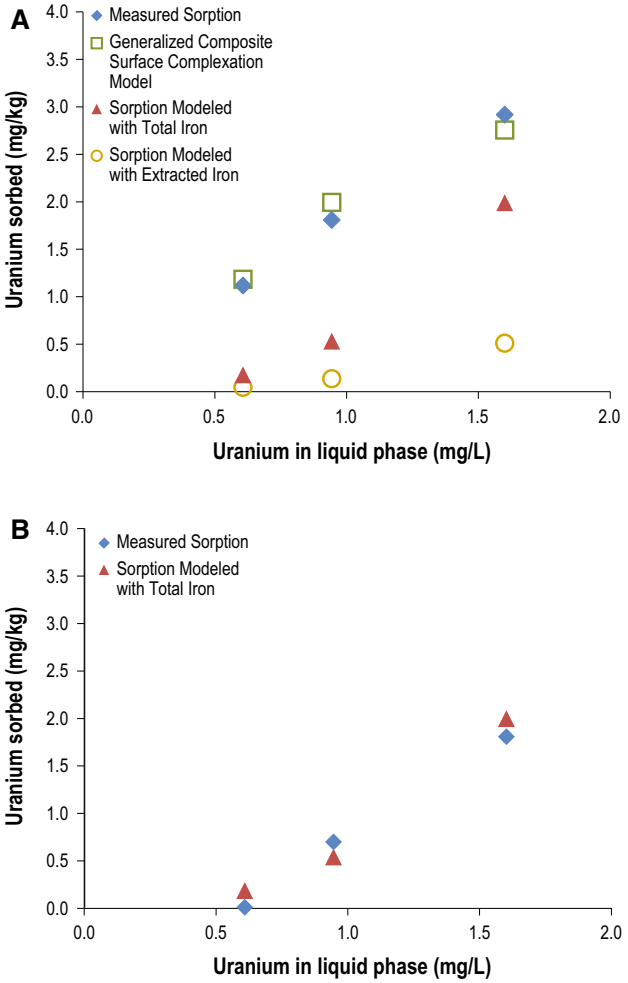

Fig. 3 Measured and modeled sorption for 11–14C–5. **a** With base sorption included. **b** Without base sorption. A *blue diamond symbol* represents the measured sorption data where the uranium in the liquid phase is plotted as the final uranium in solution from Table 2. A *red triangle* represents the modeled uranium sorption based on the total iron content and a *yellow circle* represents the modeled uranium sorption based on the total extracted iron content. The *green square* represents results from the generalized composite surface complexation models

converted to a U concentration in mg of U sorbed per kg of solid-phase sample (Table 2). The sorption coefficient (K_d) is added to Table 2 for reference. In Table 2, a negative amount of U sorbed on the solid phase indicates the amount of U originally sorbed to the sediment as received (base sorption). This base sorption was then added to the three additional batch tests with higher U concentrations. As discussed previously, this is a minimum amount of preexisting U sorption, as the full amount was not measured, so the base sorption value with the zero U spike in Table 2 was not plotted in Figs. 2, 3 and 4.

Table 2 does not include data from sample 11-14C-3 because of high dissolved vanadium concentrations (Supplemental Table A1). Whole rock data did not indicate high V concentrations for this sample (Johnson et al. 2013), so the high V in the sorption test solutions was not expected. However, other solid samples at the Dewey Burdock site have shown higher V concentrations (Johnson et al. 2013). PHREEQC simulations of the resulting solutions from sample 11-14C-3 indicate the potential for the precipitation of tyuyamunite (a low-solubility U–V oxide). Thus, data from sample 11-14C-3 do not distinguish U sorption from U precipitation, and cannot be included in sorption evaluations. For the remaining samples, PHREEQC simulations indicate that the V concentrations were below the solubility limit for tyuyamunite; there are no U–V complexes in the thermodynamic database.

In general, the sorption data in Table 2 and Figs. 2, 3 and 4 indicate increasing U sorption with increasing amounts of U in solution, as expected. For samples 11-14C-4 and 11-16C-2 (Figs. 2, 4), the sorption trends are nonlinear, and the amount of U sorbed appears to level off slightly with higher concentrations of U in solution, which indicates that there may be a maximum sorption capacity for these samples. For sample 11-14C-5, the sorption trend is more linear, which may be related to its higher total solid-phase Fe content with less total extractable Fe. This sample also has the highest base sorption amount. Overall, the total amount of U sorption (using the K_d values in Table 2) generally correlates with the amount of total extractable Fe (Table 1). A more detailed evaluation of the correlation between measured sorption and Fe content is

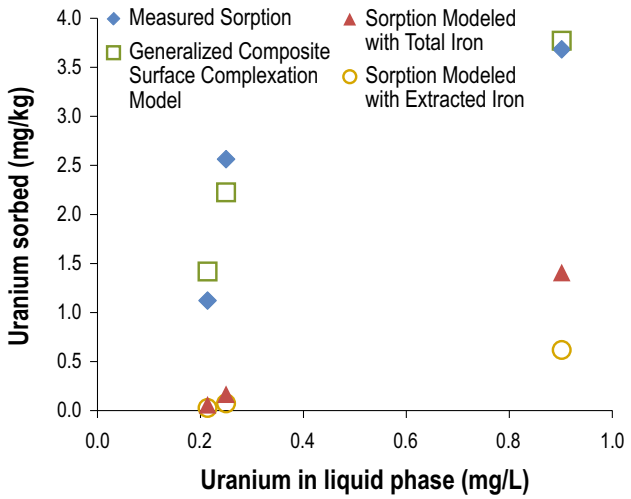

Fig. 4 Measured and modeled sorption for 11–16C–2. A *blue diamond symbol* represents the measured sorption data where the uranium in the liquid phase is plotted as the final uranium in solution from Table 2. A *red triangle* represents the modeled uranium sorption based on the total iron content, and a *yellow circle* represents the modeled uranium sorption based on the total extracted iron content. The *green square* represents results from the generalized composite surface complexation models

not straightforward because of the nonlinearity of the sorption curves.

The PHREEQC-calculated sorption with the extracted and total Fe concentrations consistently underestimates the total measured sorption of the samples (Figs. 2, 3, 4). In general, the extractable Fe would be considered to be more amorphous and might provide a greater amount of U sorption than an equivalent amount of hematite. However, the PHREEQC input for Fe is simply entered by converting to an equivalent amount of HFO. Thus, sorption differences would need to be accounted for by substantially increasing the HFO surface area beyond literature values.

The subtraction of the base sorption would have a minimal effect on the sorption curves for samples 11-14C-4 and 11-16C-5 (Table 2), but for sample 11-14C-5, the subtraction of the base sorption provides a curve that essentially matches the PHREEQC-calculated sorption curve with the total Fe (Fig. 3b). In general, it appears that the extracted Fe and total Fe contents influence the measured sorption of U but do not provide a full accounting for the total sorption capacity. Thus, the total sorption capacity is better accounted for using a generalized composite surface complexation model following the procedures of Davis et al. (2004).

Generalized Composite Surface Complexation Models

The use of generalized composite surface complexation models improves the sorption estimates (green squares in Figs. 2, 3, 4). These models provide larger sorption parameters than using Fe alone, which could significantly influence future reactive transport modeling by increasing U attenuation. Conceptually, the improved match is likely due to U sorption to clays (XRD data indicate a trace to 2 % by weight kaolinite clay content in all four samples) and other minerals present in the oxidized core samples. Actual sorption to the individual mineral types could be estimated in a component additive approach, as discussed in Davis et al. (2004). However, the research by Davis et al. (2004) indicates a better fit to their U sorption data using a generic sorption estimate with generalized composite surface complexation models. This approach honors the measured data without the need for information on the specific minerals providing the U sorption capacity.

For all three samples (excluding sample 11-14C-3 with possible mineral precipitation issues), the generalized composite surface complexation models provide the best fit when the equilibrium constants are fixed and the site densities are estimated (Table 3, S log k = 5.817 and SS log k = 6.798, plotted in Figs. 2, 3, 4), as determined by the SOSWR values calculated from PEST. The sorption curve for 11-14C-4* is discussed in the next section, "Parameter Correlation." The other parameter estimation approaches (fix site densities and estimate log k, and estimate log k and site densities using fixed ratios, Table 3) may have found local minima in the SOSWR and did not always find a more global minimum, since the SOSWR values were not as small. This is a common problem when doing parameter estimations (Doherty 2005) with nonlinear problems (Snieder 1998), which can sometimes be circumvented by using different starting parameter values. For the estimated parameters, a range of starting values were tested in an attempt to find more global minima, but they all produced the same SOSWR and final estimated parameter values listed in Table 3. In this case, it appears that the use of different parameter estimation approaches is the best way to avoid local minima, likely due to the limited number of parameters that can be estimated at once (due to having only three calibration points).

Figure 5 shows the final best-fit generalized composite surface complexation models for all three samples. Because PHREEQC uses the actual solution composition, the curves in Fig. 5 are not necessarily smooth. In Figs. 2, 3 and 4, each calibration point is a separate solution composition, whereas in Fig. 5, a solution composition had to be assigned to each additional plotted point. Thus, the jumps in the curves plotted in Fig. 5 are an artifact of using the next solution composition, which varies slightly due to small differences in the equilibrium conditions with the solid samples. This highlights the sensitivity of the U sorption to small changes in solution chemistry.

Table 3 SOSWR values for batch sorption test calibrations

Sample	S log k[a]	SS log k	S[b] site density mol/kg water	SS[c] site density mol/kg water	SOSWR[d]
	Fix log k and estimate site densities				
11-14C-4	5.817	6.798	4.539×10^{-5}	4.090×10^{-6}	0.0242
11-14C-4*[e]	1.284	1.500	1.803×10^{-1}	2.039×10^{-1}	0.5090
11-14C-5	5.817	6.798	8.036×10^{-5}	1.000×10^{-10}	0.0654
11-16C-2	5.817	6.798	7.311×10^{-5}	3.377×10^{-5}	0.2100
	Fix site densities and estimate log k				
11-14C-4	1.988	2.816	6.114×10^{-2}	6.114×10^{-3}	0.5081
11-14C-5	1.794	2.695	6.114×10^{-2}	6.114×10^{-3}	2.0310
11-16C-2	1.935	2.764	6.114×10^{-2}	6.114×10^{-3}	6.0200
	Estimate log k and site densities using fixed ratios				
11-14C-4	4.464	6.324	2.079×10^{-4}	1.873×10^{-5}	0.0879
11-14C-5	3.481	5.228	2.348×10^{-3}	2.922×10^{-9}	1.9770
11-16C-2	4.548	6.496	1.368×10^{-4}	6.318×10^{-5}	0.3906

[a] k = Equilibrium constant

[b] S = Strong

[c] SS = Super strong

[d] SOSWR = Sum-of-squared weighted residuals

[e] * = use different starting log k values to test parameter correlation

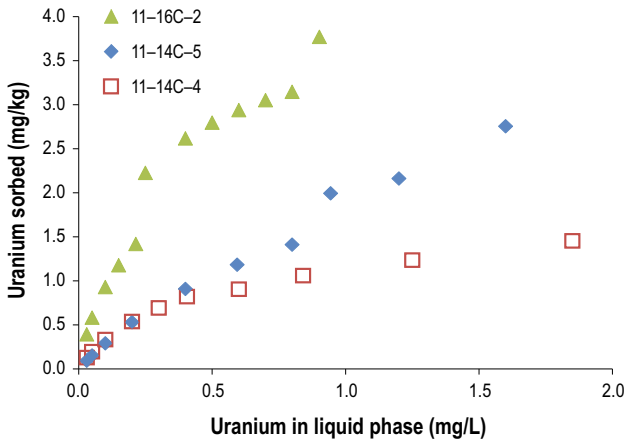

Fig. 5 Modeled sorption curves. These curves use the final sorption parameters derived from fixed equilibrium constants with estimated site densities listed in Table 3. Irregular nature of each curve is due to the slight variations in solution geochemistry for each batch sorption test (see Supplemental Table A1) that are applied to a wider range of uranium concentrations

Parameter Correlation

Output from PEST provided information on correlations between parameters, which indicated that all of the parameters are 97–100 % correlated. For the overall sorption, log k values vs site densities are 100 % inversely correlated. For sample 11-14C-4, one simulation was completed by fixing the log k numbers at lower values (but still with the same S log k to SS log k ratio), and the site densities were estimated. This simulation is indicated as 11-14C-4* in Table 3. The resulting SOSWR of 0.5090 is greater than the best fit SOSWR of 0.0242 using fixed log k values and estimated site densities, and the best-fit SOSWR could not be achieved with the fixed lower log k values. However, the SOSWR for 11-14C-4* is virtually the same as the SOSWR of 0.5081 from the fixed site densities with estimated log k trial (Table 3), which may represent a local minimum compared to the best-fit SOSWR of 0.0242 (which may be a more global minimum).

Sorption parameter correlation could lead to non-uniqueness issues in any future reactive transport modeling. For example, in groundwater flow modeling, the values for recharge and hydraulic conductivity are positively correlated, if no flow information is available (Poeter and Hill 1997). An increase or decrease in both recharge and hydraulic conductivity at the same time can produce the same match to hydraulic head values. With this, any contaminant transport predictions that use the resulting hydraulic conductivity values are non-unique, which may lead to over- or under-prediction of transport rates. For batch sorption tests, the inverse correlation between log k values and site densities and the possibility of non-unique predictions has not been tested, to the authors' knowledge. To test this non-uniqueness, a simple 1-D column was developed in PHREEQC with the site geochemistry. Groundwater was equilibrated with the solid phase using

the calibrated sorption parameters. The only change to the incoming groundwater was the addition of 0.2 mg/L U in solution, and U was allowed to sorb to the solid phase using the fixed site densities and estimated log k sorption parameters for 11-14C-4 (not the best fit, but keeps the SOSWR value similar to 11-14C-4*) and the sorption parameters for 11-14C-4*. The resulting two-column simulations cannot be visually compared because the two scenarios give the same results for U transport. However, results using the parameters from the improved fit with the fixed log k and estimated site densities for 11-14C-4 are quite different. These simple tests indicate that the non-uniqueness due to the inverse correlations between log k and site densities appears to be less important than overall calibration to the sorption curves and the resulting best-fit SOSWR values. Correlation of sorption parameters and the influence of non-uniqueness in transport predictions is an area requiring additional research.

Recommendations for Future Studies

To be more accurate, future batch sorption studies should fully leach the solid sample several times with the zero-spiked, laboratory-prepared water to get a full amount of preexisting base sorption. Alternatively, total base sorption could be determined using a carbonate leach test similar to that in Kohler et al. (2004) to determine the total amount of initially sorbed U before batch testing. In addition, the use of actual groundwater instead of a laboratory-prepared water for all of the batch testing would provide greater accuracy. However, care must be taken in preserving the groundwater when transporting it from the field to maintain its geochemistry, specifically oxygen and carbon dioxide concentrations.

In addition, having only three U concentrations for each sample limits the number of sorption parameters that can be independently calibrated. Addition of more U concentrations and variations in the water chemistry could improve the calibration efforts. Davis et al. (2004), in addition to having more U concentration values, also varied the carbon dioxide content, which in turn changed the pH. These variations allowed for the determination of more sorption parameters and allowed for calibration of these parameters over a wider range of geochemical conditions. In addition, having a significant number of rock samples from the actual downgradient area to represent the full range of expected rock types (i.e. variations in mineralogy) instead of a limited number of proxy samples would also be valuable.

The approach discussed in this paper uses batch sorption, which assumes equilibrium conditions for sorption. While this may be appropriate for certain sites, areas with faster groundwater flow and slower sorption reactions may need to consider kinetic, non-equilibrium approaches. Further investigations to evaluate possible kinetic influences could include the use of column studies with stop flow techniques to determine concentration rebound and the influence of non-equilibrium conditions.

Summary and Conclusions

We measured solid-phase Fe concentrations, conducted batch sorption tests, and developed generalized composite surface complexation models to provide sorption parameters (site densities and equilibrium constants) for a proposed U ISR site. Measured Fe concentrations did not provide a full accounting of the sorption potential but still appeared to influence the sorption characteristics of the samples. Generalized composite surface complexation models provide a method for incorporating the full sorption potential of individual samples without having to account for the full mineralogy. These generic sorption models were calibrated to the sorption data using inverse modeling, resulting in larger sorption parameters than with Fe only, which could influence future reactive transport modeling by predicting increased U attenuation. Because of the limited number of calibration points, inverse modeling required the reduction of estimated parameters by fixing two parameters, highlighting the need for additional calibration points. The best-fit models used fixed values for equilibrium constants and estimated the site densities. These inverse routines provided best-fit sorption parameters that can be used in future reactive transport modeling. However, local minima encountered during the calibration efforts must be considered when finding best-fit sorption parameters, requiring extra care in finding a more global minimum, especially with limited calibration data. The influence of correlated sorption parameters on reactive transport modeling appears to have a limited effect on the U transport results compared to the greater importance of the overall best-fit parameters, based on the SOSWR values.

Although this work focused on oxidized samples, these procedures can just as easily be applied to samples collected from a reduced zone. Additional considerations for reduced-zone samples would include proper sample collection and preservation to keep the samples anoxic, completion of laboratory tests in anoxic conditions, and additional consideration of mineral precipitation reactions beyond straight sorption.

The methods and procedures presented in this paper can potentially be applied to other sites where plans for reactive transport modeling require the appropriate estimation of metal sorption parameters as initial model input. For

proposed U ISR sites, determination of sorption parameters for use in reactive transport modeling is a necessary first step, since no other calibration data exists (i.e. no contaminant plume for transport calibration). For the Dewey Burdock site, a companion paper with site-specific reactive transport modeling and a general procedural guide for data collection (Johnson and Tutu 2016) uses the sorption parameters and information derived from this paper.

Acknowledgments Funding for this work was provided by the U.S. Geological Survey and the U.S. Department of Energy Office of Legacy Management. The authors thank Powertech (USA) Inc. for the donation of drill core for analyses. We also thank George Breit (USGS retired) for laboratory use and oversight, along with a review of this manuscript. Our appreciation also goes to Gary Curtis (USGS, Menlo Park, California) for providing the updated PHREEQC database and to the three anonymous journal reviewers for their role in improving this manuscript.

References

Adler HH (1974) Concepts of uranium-ore formation in reducing environments in sandstones and other sediments. In: Proceedings of symposium on the formation of uranium ore deposits, IAEA-SM-183/43, pp 141–168

Bachmaf S, Merkel BJ (2011) Sorption of uranium(VI) at the clay mineral-water interface. Environ Earth Sci 63:925–934

Boberg WW (2010) The nature and development of the Wyoming uranium province. In: Goldfarb RJ, Marsh EE, Monecke T (eds), The challenge of finding new mineral resources: global metallogeny, innovative exploration, and new discoveries, Ch 32, Special Publications 15, Society of Economic Geologists, pp 653–674

Borch T, Roche N, Johnson TE (2012) Determination of contaminant levels and remediation efficacy in groundwater at a former in situ recovery uranium mine. J Environ Monit 14(7):1814–1823

Clesceri LS, Freenber AE, Eaton AD (eds) (1998) 3500-Iron B. Phenanthroline method. In: Standard methods for the examination of water and wastewater, 20th edit, American Public Health Association Washington, pp 3-76–3-78

Commonwealth of Australia (2010) Australia's in situ recovery uranium mining best practice guide. Canberra

Dahlkamp FJ (2010) Black Hills. Uranium Deposits of the World, USA and Latin America, Springer, Berlin Heidelberg, Ch3, pp 209–218

Davis JA, Curtis GP (2007) Consideration of geochemical issues in groundwater restorations at uranium in-situ leach mining facilities, US nuclear regulatory commission, http://www.nrc.gov/reading-rm/doc-collections/nuregs/contract/cr6870/cr6870.pdf

Davis JA, Meece DE, Kohler M, Curtis GP (2004) Approaches to surface complexation modeling of uranium(VI) adsorption on aquifer sediments. Geochim Cosmochim Acta 68(18):3621–3641

Doherty J (2005) PEST model-independent parameter estimation, user manual. 5th edit. Watermark numerical computing, http://www2.epa.gov/sites/production/files/documents/PESTMAN.PDF

Dong W, Brooks SC (2006) Determination of the formation constants of ternary complexes of uranyl and carbonate with alkaline earth metals (Mg^{2+}, Ca^{2+}, Sr^{2+}, and Ba^{2+}) using anion exchange method. Environ Sci Technol 40:4689–4695

Dzombak DA, Morel FMM (1990) Surface complexation modeling—hydrous ferric oxide. Wiley, New York City

EPA (2011) Considerations related to post-closure monitoring of uranium in situ leach/in situ recovery (ISL/ISR) sites, draft technical report, US Environmental Protection Agency (EPA) Office of Air and Radiation, http://www.epa.gov/radiation/docs/tenorm/post-closure-monitoring.pdf

Fox PM, Davis JA, Zachara JM (2006) The effect of calcium on aqueous uranium(VI) speciation and adsorption to ferrihydrite and quartz. Geochim Cosmochim Acta 70:1379–1387

Guillaumont R, Fanghanel T, Fuger J, Grenthe I, Neck V, Palmer D, Rand MH (2003) Update on the chemical thermodynamics of Uranium, Neptunium, Plutonium, Americium, and Technetium. Elsevier, Amsterdam

Hall SM (2009) Groundwater restoration at uranium in situ recovery mines, south Texas coastal plain. USGS OFR 2009-1143, http://pubs.usgs.gov/of/2009/1143/

Harshman EN (1974) Distribution of elements in some roll-type uranium deposits. In: Proceedings, symposium on the formation of uranium ore deposits, Athens, Greece, IAEA-SM-183/4, pp 169–183

Heron G, Crouzet C, Bourg ACM, Christensen TH (1994) Speciation of Fe(II) and Fe(III) in contaminated aquifer sediments using chemical extraction techniques. Environ Sci Technol 28:1698–1705

Hobday DK, Galloway WE (1999) Groundwater processes and sedimentary uranium deposits. Hydrogeol J7:127–138

Hsi CKD, Langmuir D (1985) Adsorption of uranyl onto ferric oxyhydroxides: applications of a surface complexation site binding model. Geochim Cosmochim Acta 49:2423–2432

IAEA (International Atomic Energy Agency) (2005) Guidebook on environmental impact assessment for in situ leach mining projects. IAEA–TECDOC-1428

Johnson RH (2012) Geochemical data from groundwater at the proposed Dewey Burdock uranium in situ recovery mine, Edgemont, South Dakota. USGS OFR 2012-1070, http://pubs.usgs.gov/of/2012/1070/

Johnson RH, Tutu H (2016) Predictive reactive transport modeling at a proposed uranium in situ recovery site with a general data collection guide. Mine water environ (in this issue)

Johnson RH, Diehl SF, Benzel WM (2013) Solid-phase data from cores at the proposed Dewey Burdock uranium in situ recovery mine near Edgemont, South Dakota. USGS OFR 2013–1093, http://pubs.usgs.gov/of/2013/1093/

Kohler M, Curtis GP, Meece DE, Davis JA (2004) Methods for estimating adsorbed uranium(VI) and distribution coefficients of contaminated sediments. Environ Sci Technol 38:240–247

Mahoney JJ, Cadle SA, Jakubowski RT (2009) Uranyl adsorption onto hydrous ferric oxide—a re-evaluation for the diffuse layer model database. Environ Sci Technol 43(24):9260–9266

Nair S, Karimzadeh L, Merkel BJ (2014) Surface complexation modeling of uranium(VI) sorption on quartz in the presence and absence of alkaline earth metals. Environ Earth Sci 71:1737–1745

NRC (2009) Generic environmental impact statement for in-situ leach uranium milling facilities. US Nuclear Regulatory Commission NUREG-1910, vols 1 and 2, Final Report

NRC (2014) Environmental impact statement for the Dewey-Burdock project in Custer and Fall River counties, South Dakota. Supplement to the generic environmental impact statement for in-situ leach uranium milling facilities, US NRC Final Report, http://pbadupws.nrc.gov/docs/ML1402/ML14029A406.html

Pabalan RT, Turner DR, Bertetti FP, Prikryl JD (1998) Uranium(VI) sorption onto selected mineral surfaces: key geochemical parameters. In: Jenne E (ed) Adsorption of metals: variables, mechanisms, and model applications, Geomedia. Academic Press, San Diego, pp 99–130

Parkhurst DL, Appelo CAJ (2013) Description of input and examples for PHREEQC vers 3—a computer program for speciation, batch-reaction, one-dimensional transport, and inverse geochemical calculations. USGS techniques and methods, http://pubs.usgs.gov/tm/06/a43/

Poeter EP, Hill MC (1997) Inverse models: a necessary next step in ground-water modeling. Ground Water 35(2):250–260

Powertech (2008) Dewey-Burock project class III underground injection control permit application to the US EPA Region 8, updated January 2013, http://www2.epa.gov/region8/underground-injection-control and ftp://epa.gov/r8/DeweyBurdock/DBApplication.pdf

Powertech (2009) Dewey-Burdock project, application for NRC uranium recovery license Fall River and Custer counties, South Dakota. http://pbadupws.nrc.gov/docs/ML0928/ML092870160.html

Snieder R (1998) The role of nonlinearity in inverse problems. Inverse Probl 14:387–404

Villalobos M, Trotz MA, Leckie JO (2001) Surface complexation modeling of carbonate effects on the adsorption of Cr(VI), Pb(II), and U(VI) on goethite. Environ Sci Technol 35:3849–3856

Waite TD, Davis JA, Payne TE, Waychunas GA, Xu N (1994) Uranium(VI) adsorption to ferrihydrite: application of a surface complexation model. Geochim Cosmochim Acta 57:2251–2269